Presented at the Materials Research Society Meeting, San Francisco, CA 4/12/2007. Paper Y7-5.

Exploring Back Contact Technology to Increase CdS/CdTe Solar Cell Efficiency

Alan L. Fahrenbruch
Department of Physics, Colorado State University, Fort Collins, CO, 80523-1875

ABSTRACT

The primary routes for increasing CdS/CdTe solar cell efficiency involve increasing free carrier density, reducing bulk and interface recombination, and/or reducing back contact barrier height Φ_{bc}. This paper focuses on the role of the back contact barrier in increasing cell efficiency. Measurement of Φ_{bc} and back surface recombination are outlined and three CdTe/MX/M back contact prototypes, each with particular strengths, are discussed.

INTRODUCTION: EFFECT OF BACK CONTACT BARRIERS ON EFFICIENCY

The V_{oc} deficit ($E_g/q - V_{oc}$) for CdS/CdTe cells is large in comparison with other cells (e.g., 0.65 V for CdTe vs. 0.44 V for CIS). Optimistically, one can view this as an opportunity for increasing efficiency. There is little room for improvement in short-circuit current, so the focus here is on increasing cell voltage and fill factor. Four basic ways to do this are:

- increase free carrier density (p) in the CdTe absorber, [1]
- decrease bulk recombination, [1]
- decrease back-contact barrier height (Φ_{bc}), [2] and
- reduce back surface recombination by surface treatment and/or an electron mirror. [3]

All of these options are difficult and uncertain to do and to measure.

There is increasing evidence that the density of deep acceptors is much greater than that of shallow acceptors [e.g., 4], suggesting that the hole density p is considerably smaller than the usual $1/C^2$ vs. V measurements indicate ($\approx$ 3e14 cm^{-3}).

The experimental correlation between bulk recombination lifetime and real cell efficiency for CdS/CdTe has only recently become quantitative, when Metzger et al. [5] found a positive correlation between lifetime measured by Transient Photoluminescence and V_{oc}. While the experimental connections between fabrication variables and efficiency are strong, a description in terms of specific defect species and their recombination properties is still under discussion and device modeling is still somewhat tentative [6].

This paper focuses on the role of the back contact barrier. This is perhaps the most uncertain choice for increasing V_{oc} for thin cells, but arguably it has the highest potential payoff, especially if applied in combination with decreased bulk recombination.

For electronically thick cells ($X_{CdTe} > \approx 2\ W_d$, where X_{CdTe} is the CdTe thickness and W_d the depletion layer width), the depletion layers of the main junction and the back contact don't overlap and the back contact can be treated as a series-opposing Schottky barrier. For values of $\Phi_{bc} \leq 0.3$ eV, ff and V_{oc} aren't substantially affected. Increasing Φ_{bc} beyond 0.3 eV mainly decreases ff with a small loss of V_{oc}. [7,8].

However, the cost-driven trend is toward thinner CdTe layers. Modeling suggests that efficiency gains due to decreased back-contact barrier height Φ_{bc} become greater for thinner CdTe and smaller space charge density SCD. Given the low SCD values observed, thin cells are generally nearly or completely depleted at zero bias. They behave more like n/i/p junctions, in which the built-in voltage is established by the front and back contacts and V_{oc}, ff, and J_{sc} become almost independent of p. Because of the large built-in electric fields n/i/p devices are more tolerant of small minority carrier lifetimes [1,3]. Modeling shows that V_{oc} in thin CdS/CdTe cells is inversely related to the back-contact barrier height Φ_{bc}.

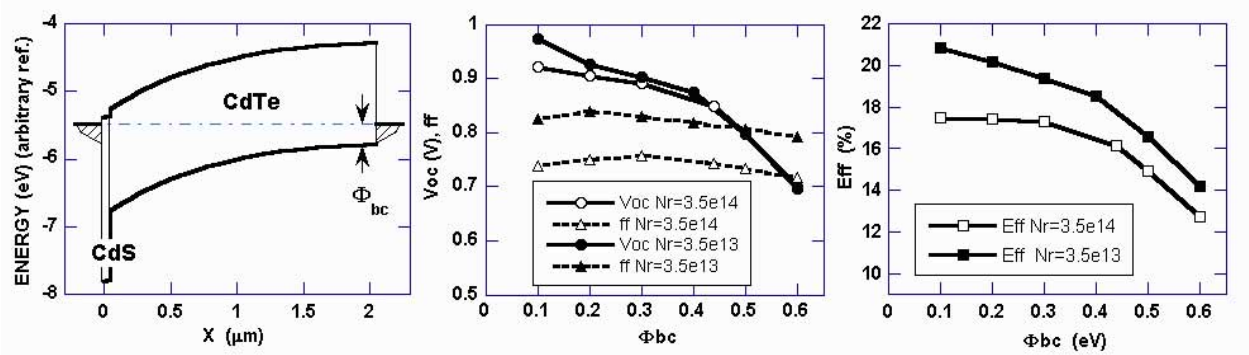

Figure 1. Model results for n/i/p CdS/CdTe device with CdTe acceptor density N_a = 3e14 cm^{-3}, E_a = 0.3 eV: (a) band diagram, (b) V_{oc}, ff vs. Φ_{bc}, for two recombination center densities (N_r, donors and acceptors at $E_r = E_v + 0.75$ eV). Large back surface recombination velocities $S_{bc,n} = S_{bc,p}$ = 1e7 cm/sec are assumed. J_{sc} is nearly constant at ≈ 25 mA/cm^2. (c) Efficiency vs. Φ_{bc}.

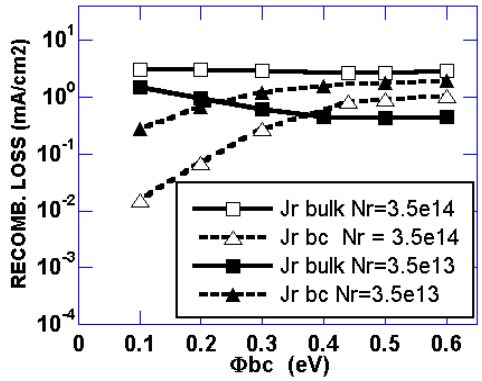

Figure 2. Modeled bulk and back contact recombination loss currents vs Φ_{bc} for cell of figure 1 at the maximum power point. $S_{bc,n} = S_{bc,p}$ = 1e7 cm/sec. are assumed.

Figure 1 indicates that the major increase in efficiency for smaller Φ_{bc} is due to an increase in V_{oc} rather than an increase in ff. Figure 2 shows recombination loss for the bulk ($J_{r,bulk}$) and at the back contact ($J_{r,bc}$). $J_{r,bc}$ is ~ q n S_{bc}, where n is the electron density and S_{bc} is the recombination velocity at the back contact. For small Φ_{bc}, < 0.2 eV, the electron density at the contact is extremely small, so even large S_{bc} has little effect on the efficiency. For Φ_{bc} > 0.2 eV, $J_{r,bc}$ becomes large and an electron mirror such as p-ZnTe would be needed to maximize efficiency [1].

A compelling reason for focusing on Φ_{bc}, is that the back contact is a troublesome issue in existing technology, reducing cell repeatability, uniformity, and stability.

A major practical advantage to manipulation of Φ_{bc}, rather than bulk properties, is that the back contact is accessible to surface processing, greatly aiding combinatorial searches for better contacts.

BACK-CONTACT BARRIER MEASUREMENTS

It must be emphasized that the CdS/CdTe cell is a highly interdependent system, and so it can be misleading to look at the back contact in isolation. For example, it is usual to associate J-V curve roll-over with the back contact. However, J-V roll-over can arise from five different sources: parasitic series resistance, CdS (photo-conductivity pc [8a]), bulk CdTe (pc [8a]), bulk CdTe (space-charge-limited current [8b]), and/or the back contact (reverse Schottky barrier [7]). For thin CdTe, there may be photoconductivity effects at the back contact, as well. Thus, apparent contact results can arise from variations in bulk defect density or CdTe thickness.

Measurement of Φ_{bc}

Methods of measurement of Φ_{bc} are shown in table I.

For layers with an ohmic contact on one side, several methods are available and results are direct and accurate, IPE being perhaps the best in this regard.

For completed devices, the choices are few and results are sometimes ambiguous. In cells with electronically thick CdTe, the J-V roll-overs above V_{oc} in both dark and light are usually similar in magnitude. Arrhenius plots of experimental J at V > V_{oc} or of the apparent series

resistance give reasonable values, typically ≈ 0.3 – 0.5 eV for good cells [7,9,10]. For model results, Arrhenius plots of J at $V > V_{oc}$ for these thick devices are usually self-consistent with the Φ_{bc} values used in the model.

Table 1. Measurement of Φ_{bc}

Single Layer	Device
Diode J_o vs 1/T	$J(V>V_{oc})$ vs. 1/T
Internal photoemission IPE	UPS & XPS
$1/C^2$ vs V extrapolation	AS vs. T
Contact resistivity (TLM) vs. 1/T	
Kelvin, CPD to measure changes	
Surface photovoltage SPV	
UPS & XPS	
Ballistic electron energy microscopy BEEM	

For thin n/i/p-like junctions, the role of Φ_{bc} changes radically, and roll-over occurs mainly in the dark. In these cases, modeling suggests that the $J(V>V_{oc})$ vs 1/T analysis doesn't work; the results are controlled by the temperature and illumination dependencies of p in the CdS and CdTe bulk layers. For example, for the model of figure 1, in the dark, setting Φ_{bc} = 0.1 eV (or 0.6 eV) gives activation energies of 0.29 eV (or 0.46 eV) for the rollover of J at 1 V.

UPS and XPS are powerful surface sensitive techniques to determine band discontinuities and barrier heights and they are arguably the most direct for devices. They probe very small depths from the surface < 30 Å, so to determine barrier heights they must be employed during growth of the device structure by layer build up (or removal, by sputtering) [11,11a]. Hence UPS results may not be directly applicable to devices fabricated under typical lab conditions.

Kelvin contact potential [12] and surface photovoltage SPV [13] are sensitive non-contact methods to measure changes in barrier height. Ballistic Electron Energy Microscopy, BEEM, uses an STM tip to obtain barrier height images with ~ 10 nm resolution [13a,b,c]. In scanning mode, these methods could be particularly valuable in combinatorial searches for better contacts.

A relatively unexplored method is admittance spectroscopy AS. Using AS, Nollet [14] finds activation energies of 0.4 to 0.5 eV for several cells, depending on Au or Mo contact preparation, which they attribute to the back contact. Modeling of devices with different Φ_{bc} (but otherwise identical), does show a strong effect on capacitance-frequency data, but it appears to be formidably complex to extract Φ_{bc} numbers from C-f data for real cells.

Despite the obvious importance of Φ_{bc} data and its value as feedback to fabrication, it is scarce for polycrystalline PX thin CdTe films and devices, with few measurements on good cells.

Back Contact Recombination

The back-contact recombination loss J_{bc} depends on the interface recombination velocities $S_{bc,n}$ and $S_{bc,p}$ (determined by the interface recombination center densities and their cross sections and energy levels), and exponentially on Φ_{bc}.

Measurement of S_{bc} is indirect and requires well thought out models to separate surface from bulk recombination losses. Illumination through the contact is usually required. Methods include spectral response of surface photovoltage (SPV) [15], photo-acoustic spectroscopy [16], Photothermal Deflection (PDS) [17], and transient optical grating techniques [18]. Several of these references report strong sensitivity to surface treatment, promising reduction of J_{bc} by chemical modification of the interface.

CdTe/METAL AND CdTe/DIPOLE/METAL PROTOTYPES

Ideally, the Φ_{bc} of a CdTe/metal contact would depend only on the electron affinity χ of the CdTe and the metal work function (the Schottky limit) (figure 3a). However, CdTe is mostly covalent so Φ_{bc} is dominated by interface states, and depends only weakly on the metal work function. This is illustrated in table II for single-crystal (SX) CdTe [e.g., 11].

Table II. Barrier Heights ($E_F - E_{vb}$)

Metal	χ(eV)	Schottky Limit Φ_b (eV)	Observed Φ_b (eV)
Pt	5.6	0.2	1.0
Au	5.1	0.7	0.85
Cc	4.2	1.6	1.18

We can describe several different barrier heights:
• the Schottky limit values given by the CdTe electron affinity and the metal work function, and
• the observed barrier height measured by IPE or CV for CdTe/M diodes. These are sensitive to preparation, suggesting the possibility of purposeful chemical modification.

One explanation of this apparent contradiction is that it is really a CdTe/dipole/M junction (figure 3b), where the interface states result in an atomic scale dipole between the semiconductor and metal to give an apparent effective electron affinity smaller than that of the bulk. Such a dipole is only several atoms thick, so tunneling doesn't impede carrier transport. Its magnitude depends on what defect states were formed by the interface reaction [11a]. (The dipole in the simulation of figure 3b was created by adding 5e12 cm^{-2} acceptors at E_a = 0.45 eV (an acceptor level commonly observed in PX CdTe) near the surface.) Since these contacts are generally made without subsequent heat treatment, in-diffusion of dopants into the CdTe is unlikely.

The Φ_{bc} for the CdTe/dipole/-Metal contacts above is still much too high for good solar cells), so there is a device limit from observed cell J-V curves; Φ_{bc} must be 0.35 to 0.45 eV or less. Evidently contact processing, such as etching and heat treatment, either introduces tunneling states just inside the bulk, or further alters the dipole, in which case tunneling doesn't impede carrier transport.

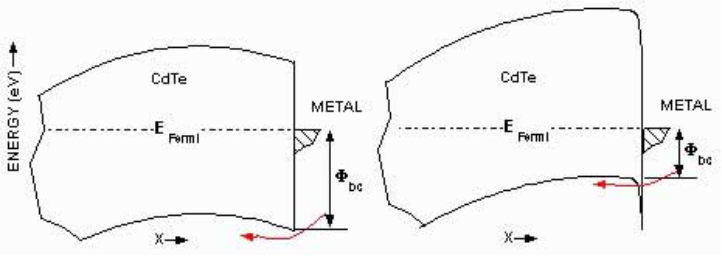

Figure 3. Junctions: (a) CdTe/M, (b) CdTe/Dipole/M. Dipole thickness (0.1 μm in simulation) is exaggerated for clarity.

There appears to be a continuum between (1) creation of high densities of acceptors within the CdTe bulk (e.g., by diffusion of Cu), with consequent tunneling transport, and (2) formation or alteration of a layer of acceptor-like interface states (e.g., by etching to produce V_{Cd}, or by reaction with metal) which forms a dipole to change the effective χ. Such pinning has been discussed by Shaw [36], for CdTe, and more generally, by Tung [20].

The dipole explanation seems more valid, because self-compensation in the CdTe works against achieving the doping density required for tunneling, and such densities have not been observed in PX CdTe.

SX p-CdTe surface treatment with n-butyllithium [19] gives p^+ layers ≈ 80 nm thick with p ≈ 3e19 cm^{-3} yielding contact resistivities as low as 0.01 Ω-cm^2. This is a macroscopic example of the dipole exercise above. Unfortunately the Li contact is only stable for a few months.

There is extensive literature on other means of altering χ and/or band bending of CdTe surfaces by surface modification. Certainly, etching steps (usually creating thin Te layers) are critical for most of the contacting schemes, even when subsequent semiconductor layers are applied (next section).

More aggressive surface modifications, such as ion bombardment of the CdTe surface have been found to drastically alter the J-V characteristics of subsequent CdTe/M contacts. Gurumurthy [20a] found large improvements in the characteristics of Au/n-CdTe (SX) diodes on exposure to N plasma before Au deposition (e.g. J_o went from 4.4e-8 to 1.6e-12 A/cm^2 and A from 1.6 to 1.1, where J_o is the diode pre-exponential and A the ideality factor). Substantial changes in χ of PX CdTe by adsorption of organic molecules such as dicarboxylic acid, with a rational dependence on the dipole moment of the adsorbant, have been observed [21]. Another

example is N-methyl benzohydroxamic acid [26a]. Unfortunately, the effect of organic molecules on cell properties so far has been largely negative.

CdTe/MX/METAL PROTOTYPES

Introducing an MX layer (MX = Cu_xTe, ZnTe, Sb_2Te_3, Ni_2P, Te [22], etc.) adds additional flexibility for E_g and χ, but adds another junction and another barrier height, figure 4. Dipole layers at both the CdTe/MX and MX/metal interfaces are likely to be present. A high SCD in the MX, to allow tunneling to the metal at the MX/M junction, and a high p, to reduce Φ_{bc} at the CdTe/MXs junction, are required. Finally, we need either a dipole modification or an in-diffusion of acceptors to produce tunneling states at the CdTe/MX interface.

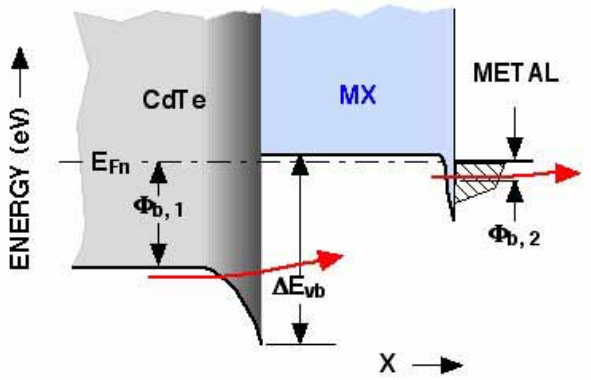

Figure 4. CdTe/MX/M contact expanded.

MX = Cu_xTe

By far the most widely used CdTe contact involves Cu_xTe. A thin Te layer, formed by etching the CdTe or by Te deposition, is then converted to Cu_xTe by in-diffusion of Cu, either from a paste containing Cu or from deposition of Cu. [10] (figure 5, assuming Φ_{bc} = 0.45 eV.). The highest efficiencies for CdTe cells have been achieved with Cu_xTe layers by Wu [23, J_{sc} = 25.9 mA/cm^2, V_{oc} = 0.845, ff = 0.755, Eff = 16.5%] and Britt and Ferekides [24].

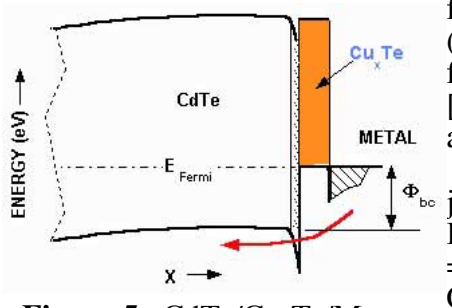

Figure 5. CdTe/Cu_xTe/M.

The high p in Cu_xTe allows tunneling at the Cu_xTe/metal junction, so many different M layers can be used (Al, Ni, Cr, ITO, graphite, etc.) [25]. Farag [26] found a direct band gap = 1.18 eV for Cu_xTe with x ≈ 1.98, and p ≈ 1e21 cm^{-3} due to Cu vacancies. Späth et al. [27], using UPS measurements during growth of Cu_xTe contacts with 1.5 < x < 1.9, found E_g = 1.04 eV and Φ_{bc} = 0.7 to 0.8 eV (depending on p). This Φ_{bc} is much larger than indicated by cell J-V measurements. They concluded that contact transport was by tunneling through the CdTe/CuxTe barrier, and involved Cu states in the CdTe.

Wu et al. [23] found that control of the amount of Cu was critical for the contact, and a mixed phase of x = 1 and 1.4 gave the best PV parameters. From log J(V > V_{oc}) vs 1/T they found Φ_{bc} = 0.48 eV.

However, Cu is a mixed blessing. Cu is lost by diffusion into the bulk and by oxidation at the surface. Most of the Cu diffused into the bulk finds its way to the CdS, lowering its SCD, and causing it to become photoconductive. While this causes light/dark J-V cross-over and roll-over mostly in the dark, it doesn't necessarily compromise cell efficiency. The effect of Cu in the CdTe is more problematic, both adding recombination centers (to lower efficiency) and increasing the SCD, which might either raise or lower efficiency, depending on CdTe thickness. Naively, it should have less effect for thin n/i/p cells.

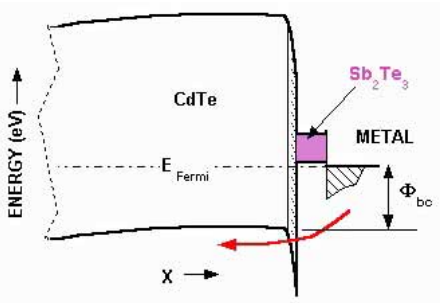

Figure 6. CdTe/Sb_2Te_3/M.

MX = Sb_2Te_3

A number of researchers have sought contacts not involving Cu, including Sb_2Te_3 and Ni_2P [28]. Sb_2Te_3 has a small band gap ≈ 0.2 eV. Deposited at low temperature, it is

amorphous and resistive, but at higher temperatures, it crystallizes, and carrier densities increase with substrate temperature (to p ≈ 1e20 cm^{-3}). A value of χ can't be found, so in figure 6, χ and a dipole are assumed to make Φ_{bc} = 0.45 eV, the largest Φ_{bc} suggested by J-V data.

Using Sb_2Te_3, Romeo et al. [29, 29a] obtained high efficiency, and their preliminary results indicate greater stability than for devices with contacts involving Cu (V_{oc} = 0.862, ff = 0.72, Eff = 15.8%). Their 100 nm Sb_2Te_3 layers are deposited by sputtering at a high substrate temperature (300°C). There appears to be no evidence of Sb diffusion doping of the CdTe, suggesting formation of an interface dipole. Other researchers [e.g., 30] have obtained only moderate PV results with Sb_2Te_3, possibly because of low p in the Sb_2Te_3.

It has been argued that there is still residual Cu from the raw materials (CdTe and $CdCl_2$), but the amount of Cu roaming in the cell is certainly reduced, and this reduction may ultimately provide greater efficiency and stability, given proper optimization of the contact.

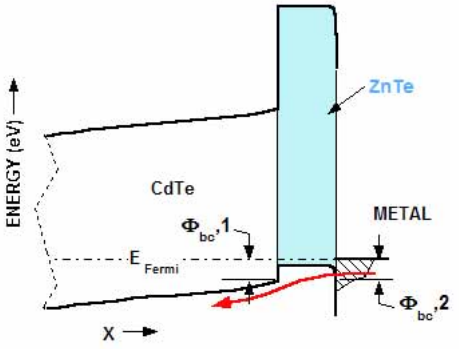

Figure 7. CdTe/ZnTe/M junction

MX = ZnTe

A third example is p-ZnTe, with a favorable valence band discontinuity $\Delta E_{vb} \approx 0$ to 0.1 eV [31,32]. For PX films, N or Cu doping can be higher than 5e18 cm^{-3} [e.g., 33], which is enough to allow tunneling to an outer metal contact (figure 7). In addition, ZnTe appears to have a lower Φ_b to the metal than does CdTe.

Extensive research on ZnTe doped with Cu has been done by Gessert et al. [34, Eff = 12.1%] and Tang et al. [35, Eff = 12.9%]. Hall effect hole densities [35] were in the range 1e19-1e20 cm^3 for films with [Cu] = 2 to 6 at. %. ZnTe:Cu does make a low resistance contact, although the control of the Cu diffusing into the bulk CdTe and CdS is critical [34].

Makhratchev et al. [33] did preliminary stability studies comparing cells with ZnTe:N and Cu/Au contacts, finding that Cu efficiencies start higher, but ZnTe:N degradation is smaller and final efficiencies are higher.

Provided that the SCD in the ZnTe is indeed high, and given the low ΔE_{vb} at the CdTe/ZnTe interface, a low Φ_{bc} is indicated, with consequently low electron density at the contact. This, in itself, should reduce back surface recombination loss at the maximum power point to negligible values for this system, even for a high interface recombination velocity S_i. This suggests that roll-over observed in experimental J-V curves [e.g., 34] may be due to other causes such as (a) photoconductivity in the CdS or CdTe, (b) space-charge limited current in the CdTe, (c) formation of a donor dipole layer at the CdTe/ZnTe interface, or (d) insufficient carrier density in the ZnTe for tunneling at the ZnTe/M interface.

DISCUSSION

The Φ_{bc} values determined by UPS and XPS are generally much higher than would be expected from J-V data for real devices [11a]. For example, Späth et al. [27] find Φ_{bc} = 0.7 - 0.8 eV for Cu_xTe contacts, whereas good PV devices admit only Φ_{bc} values < 0.3 to 0.4 eV. Some possible explanations for this apparent contradiction are:

(a) Tunneling through the barrier would require increasing the SCD to ≈1e18 cm^{-3} in the CdTe, unlikely given the strong propensity of CdTe toward bulk self-compensation. Why such high doping could be obtained near the contact, whereas even modest doping (≈1e16 cm^{-3}) is unachievable in the PX bulk, is an open question. Regions of high p haven't been reported in UPS and XPS measurements, to the best of my knowledge. A somewhat more reasonable alternative is step-wise tunneling and recombination through high densities of defect states, perhaps introduced by interface reactions.

(b) CdTe surfaces may have multiple pinning energies [36], so modification of Φ_{bc} by changes in the interface state dipole at the contact, due to subsequent processing, seems more reasonable than invoking tunneling.

(c) The Φ_{bc} values determined by UPS and other laboratory methods may not be representative of those obtained in conventional fabrication. Most MX conductivity measurements report very high p (usually determined by vacancy density), whereas some of the UPS studies find nearly intrinsic MX or Te [22]. The character of MX may also change with thickness e.g., from amorphous to crystalline. The MX's described have SCD determined by vacancies, so MX stoichiometry may not be the same. Also, the etching step is critical to most procedures, and that may be different

(d) Scanning techniques (e.g., BEEM [13b,c] and cathodoluminescence [37]) reveal strong two dimensional variations of Φ_{bc} in SX CdTe [13b,c] and PX CdTe [37]. Grain boundaries, as perpendicular extensions of the contact interface, would contribute to these Φ_{bc} distributions. High field regions, resulting from interface topology, grain boundary intersections with the contact interface, or from non-uniform interface reactions [22] would also contribute to variations in Φ_{bc}. UPS, C-V, and IPE measure the average of Φ_{bc} over area, whereas contact transport and thermionic emission are heavily weighted to the minimum of a Φ_{bc} distribution.

An excellent, in-depth review of these concepts is given by Tung [20].

CONCLUSIONS

For thin cells modeling predicts sizeable efficiency increases for lower barrier heights.

Measurement techniques for barrier height are precise and direct for layers, but indirect and sometimes ambiguous for devices. Photoelectron spectroscopy measurements give barrier height values considerably higher than indicated for good cells, perhaps due to differences in fabrication or two dimensional variations in Φ_{bc}. The latter is a particularly important issue.

However, great strides have been made in fundamental studies of these contacts, particularly with UPS and XPS, which remain the most sensitive and direct methods for devices. Barrier height data for devices is very scarce and so continued fundamental, in-depth measurements, both on layers and completed devices, are needed

In the past most contacts were found with a large amount of trial and error. And, given the complexity of finding new contacts, an intelligent, Edisonian trial and error approach is also needed to explore existing contacting procedures, and to search for new ones. The use of combinatorial approaches to finding new contact materials, perhaps using Kelvin and SPV probes, would be invaluable. These could include variations in the CdTe surface stoichiometry.

An important part of finding a good back contact is being able to measure it accurately. J-V curve roll-over can be a misleading measure of contact resistance and Φ_{bc}, especially with thin n/i/p devices. So more direct methods of measurement need to be developed, both for prototype contacts and completed devices.

ACKNOWLEDGEMENTS

The author thanks Brian McCandless, Piero Pianetta, and Jim Sites for helpful discussions. This research was supported by the U.S. National Renewable Energy Laboratory. Modeling results were obtained using AMPS-1D (Version 1,0,0,1), by S. Fonash, Pennsylvania State Univ., with EPRI support, and SCAPS 2.4 by M. Burgelman, ELIS, Univ. of Gent, Belgium.

REFERENCES

1. J. Sites and J. Pan, E-MRS (06), Nice. Thin Solid Films (07), in press.
2. A. Fahrenbruch, **4**th World Conf. Photovoltaic Energy Conversion, Hawaii (06) p.376.
3. P. V. Meyers, Solar Cells **27**, 91 (89).
4. U. Reislöhner, M. Hädrich, et al., E-MRS (06). Thin Solid Films (07), in press.

5. W. K. Metzger, M. J. Romero, P. Dippo, and M. Young, **4**th World Conf. Photovoltaic Energy Conv., Hawaii (06) p. 372.
6. M. Burgelman, J. Verschraegen, S. Degrave, P. Nollet Thin Solid Films **480-1**, 392 (05).
7. A. Niemegeers and M. Burgelman, J. Appl. Phys., **81**, 2881 (97).
8. S. H. Demtsu and J. R. Sites, Thin Solid Films **510**, 320 (06).
8a. G. Agostinelli, E. D. Dunlop, D. L. Bätzner, A. N. Tiwari, P. Nollet, M. Burgelman, and M. Köntges, **3**rd World Conf. Photovoltaic Energy Conv., Osaka (03) p. 356.
8b. Some experimental J-V characteristics can be fitted precisely by $J = J_o(V-V_o)^2$, where V is the applied bias and J_o and V_o are constants.
9. G. Stollwerck and J. R. Sites, **13**th European PV Solar Energy Conf., Nice, (95), p. 2020.
10. B. E. McCandless and J. Phillips, J. Titus, 2nd World PVSEC Conf., Vienna, (98), p. 448.
11. A. Klein, "*Advances in Solid State Analysis,*" **44,** Springer (04) p. 13.
11a. A. Klein, F. Sauberlich, B. Späth, T. Schulmeyer, & D. Kraft, J. Mater. Sci. **42**, 1890 (07).
12. D. Schroder, "*Semiconductor Material & Device Characterization*," Wiley (06) p. 526, 550.
13. L. Kronik and Y. Shapira, Surf. Interface Anal. **31**, 954 (01). Also, Schroder op cit. p. 404.
13a. V. Narayanamurti and M. Kozhenvnikov, Physics Reports **349**, 447-514 (01).
13b. I. M. Dharmadasa, Prog. in Crystal Growth and Character. of Mat'ls. **36**, 249-290 (98).
13c. A. E. Fowell, R. H. Williams et al., Semicond. Sci. Technol. **5**, 346 (90).
14. P. Nollet, M. Burgelman, S. Degrave, and J. Beier, Proc. **28**th IEEE Photovoltaic Specialists Conf. (02). p. 704.
15. J. Tousek, D. Kindl, J. Tousˇkova´, S. Dolhov, and A. Poruba, J. Appl. Phys. **89**, 460 (01).
16. M. A. Gonzalas et al., J. Phys. IV France **125** 411 (05).
17 P. Grunow and M. Kunst, J. Appl. Physics **77**, 2767 (95).
18. V. Mizeikis, K. Jarasiunas, N. Lovergine, and K. Kuroda, Thin Solid Films **364** 186 (00).
19. C-T. Lee and R. H. Bube, J. Appl. Phys. **54**, 7041 (83).
20. R. T. Tung, Materials Science and Engineering Reports **35**, 1-138 (01).
20a. S. Gurumurthy, H. L. Bhat, and V. Kumar, Semicond. Sci. Technol. **14**, 909 (99).
21. I. Visoly-Fisher, A. Sitt, M. Wahab, and D. Cahen, ChemPhysChem, **6**, 277 (05).
22. D. Kraft, A. Thissen, J. Broetz, S. Flege, M. Campo, A. Klein, and W. Jaegermann, J. Appl. Phys. **94**, 3589 (03).
23. X. Wu, J. Zhou, A. Duda, Y. Yana, G. Teeter, S. Asher, W. K. Metzger, S. Demtsu, S.-H. Wei, R. Noufi, **17**th E-PSEC (06), Munich. Thin Solid Films (07), in press.
24. J. Britt and C. Ferekides, Appl. Phys. Lett. **62**, 2851 (93).
25. S. S. Hegedus and B. E. McCandless, Solar Energy Materials and Solar Cells **88**, 75 (05).
26. B. S. Farag et al. Thin Solid Films **201**, 231 (91) and . **247**, 112 (94).
26a. M. Bruening et al. J. Am. Chem. Soc. **116**, 2977 (1994).
27. B. Späth et al., E-MRS (06), Nice. Thin Solid Films (07), in press.
28. V. Viswanathan et al., Proc. **28**th IEEE Photovoltaic Spec. Conf., (00) p. 587.
29. N. Romeo, A. Bosio, and V. Canevari, Solar Energy **77**, 795 (04).
29a. D. L Batzner et al., Thin Solid Films **451**, 536 (04).
30. K. Barri, M. Jayabal, H. Zhao, D. L. Morell, S. Asher, J. W. Pankow, M. R. Young, and C. S. Ferekides, Proc. **31**st IEEE Photovoltaic Spec. Conf., (05) p. 287.
31. D. Rioux, S. W. Niles, and H. Hochst, J. Appl. Phys. **73**, 8381 (93).
32. B. Späth, J. Fritsche, A. Klein, and W. Jaegermann,.Appl. Phys. Lett. **90**, 62112 (07).
33. K. Makhratchev, K. J. Price, X. Ma, D. A. Simmons, J. Drayton, K. Ludwig, A. Gupta, R. G. Bohn, A. D. Compaan, Proc. **28**th IEEE Photovoltaic Spec. Conf., (00) p. 475.
34. T. A. Gessert, S. Asher, S. Johnson, A. Duda, M. R. Young, and T. Moriarty, **4**th World Conf. Photovoltaic Energy Conv., Hawaii (06) p. 432.
35. J. Tang, D. Mao, T. R. Ohno, V. Kaydanov, and J. U. Trefny, Proc. **26**th IEEE Photovoltaic Specialists Conf. (97). p. 439.
36. J. L. Shaw et al., J. Vac. Sci. Technol. **A6**, 2752 (88).
37. P. Sutter; E. Sutter, and T.R. Ohno, Applied Physics Letters; **84**, 2100 (04).